JOURNAL

OF THE AMERICAN CHEMICAL SOCIETY

VOLUME 109, NUMBER 19 SEPTEMBER 16, 1987

Theoretical Studies of Transition-Metal Hydrides. 3. SrH^+ through CdH^+

J. Bruce Schilling, William A. Goddard III,* and J. L. Beauchamp

Contribution No. 7551 from the Arthur Amos Noyes Laboratory of Chemical Physics, California Institute of Technology, Pasadena, California 91125. *Received February 13, 1987*

Abstract: Generalized valence bond plus configuration interaction calculations have been carried out on the monopositive diatomic metal hydride ions of the second transition-metal series (YH^+–CdH^+, including SrH^+). We analyze the trends in bond energies, equilibrium geometries, vibrational frequencies, and metal orbital hybridizations. The trends in these quantities can be understood in terms of (1) the low-lying electronic states of the metal, (2) the orbital sizes of the metal, (3) the loss of exchange energy on bonding to the high-spin metal, and (4) the intrinsic bond strengths of bonding H to metal 5s and 4d electrons. We also present bond lengths, vibrational frequencies, and relative energies for selected MH^+ excited states.

I. Introduction

Recent studies of gas-phase transition-metal ion chemistry have focused on determination of the differences in reactivity of the various metal ions with small organic and inorganic molecules,[1] structural determination of reaction products,[2] investigation of reaction mechanisms,[3] and attempts to unravel the differences in reactivity between ground- and excited-state species.[4] Central to analyzing such chemical reactivity studies is an understanding of various thermodynamic quantities, particularly the metal–ligand bond dissociation energies. In order to determine the factors affecting σ bonding in metal ion systems, we have performed systematic theoretical studies of the bonding in the first- and second-row transition-metal hydride ions. Presented here are the results for the second-row systems, the first-row results having been published previously.[5]

(1) See, for example: (a) Armentrout, P. B.; Halle, L. F.; Beauchamp, J. L. *J. Chem. Phys.* **1982**, *76*, 2449. (b) Halle, L. F.; Crow, W. E.; Armentrout, P. B.; Beauchamp, J. L. *Organometallics* **1984**, *3*, 1694. (c) Jacobson, D. B.; Freiser, B. S. *J. Am. Chem. Soc.* **1983**, *105*, 7492. (e) Jacobson, D. B.; Freiser, B. S. *J. Am. Chem. Soc.* **1983**, *105*, 5197. (f) Cassady, C. J.; Freiser, B. S. *J. Am. Chem. Soc.* **1985**, *107*, 1573. (g) Babinec, S. J.; Allison, J. *J. Am. Chem. Soc.* **1984**, *106*, 7718.

(2) See, for example: (a) Larsen, B. S.; Ridge, D. P. *J. Am. Chem. Soc.* **1984**, *106*, 1912. (b) Jacobson, D. B.; Freiser, B. S. *J. Am. Chem. Soc.* **1983**, *105*, 736.

(3) See, for example: (a) Halle, L. F.; Houriet, R.; Kappes, M. M.; Staley, R. H.; Beauchamp, J. L. *J. Am. Chem. Soc.* **1982**, *104*, 6293. (b) Houriet, R.; Halle, L. F.; Beauchamp, J. L. *Organometallics* **1983**, *2*, 1818. (c) Hanratty, M. A.; Paulsen, C. M.; Beauchamp, J. L. *J. Am. Chem. Soc.* **1985**, *107*, 5074.

(4) (a) Halle, L. F.; Armentrout, P. B.; Beauchamp, J. L. *J. Am. Chem. Soc.* **1981**, *103*, 962. (b) Elkind, J. L.; Armentrout, P. B. *J. Phys. Chem.* **1985**, *89*, 5626. (c) Elkind, J. L.; Armentrout, P. B. *J. Chem. Phys.* **1986**, *84*, 4862. (d) Elkind, J. L.; Armentrout, P. B. *J. Am. Chem. Soc.* **1986**, *108*, 2765.

(5) (a) Schilling, J. B.; Goddard, W. A., III; Beauchamp, J. L. *J. Am. Chem. Soc.* **1986**, *108*, 582. (b) Schilling, J. B.; Goddard, W. A., III; Beauchamp, J. L., submitted for publication.

Table I. Character of Wave Functions for MH^+ (from GVB-PP Calculations)

molecule[a]	state	character of metal bonding orbital % s	% p	% d	overlap	charge transfer to H
SrH^+ (d^0)	$^1\Sigma^+$	56.3	14.2	29.5	0.755	0.25
YH^+ (d^1)	$^2\Sigma^+$	31.9	10.2	57.9	0.760	0.25
ZrH^+ (d^2)	$^3\Phi^\pm$	36.0	10.6	53.4	0.757	0.17
NbH^+ (d^3)	$^4\Delta^\pm$	30.0	9.3	60.7	0.743	0.13
MoH^+ (d^4)	$^5\Sigma^+$	19.7	7.0	73.3	0.703	0.09
TcH^+ (d^5)	$^6\Sigma^+$	40.5	7.0	52.5	0.751	0.11
RuH^+ (d^6)	$^3\Sigma^-$	9.0	3.9	87.1	0.622	−0.05
RhH^+ (d^7)	$^2\Delta^\pm$	7.0	3.0	90.0	0.595	−0.09
PdH^+ (d^8)	$^1\Sigma^+$	5.1	2.1	92.8	0.572	−0.12
CdH^+ (d^{10})	$^1\Sigma^+$	90.4	9.2	0.4	0.674	0.04

[a] Nonbonded d orbital occupation given in parentheses.

II. Results and Discussion

Character of the Wave Function. Figures 1 and 2 show the generalized valence bond (GVB) bond orbitals for SrH^+ through CdH^+ (excluding AgH^+). The GVB orbitals for the bond pairs involve an orbital with one electron centered on the metal ion and an orbital with one electron located on the hydrogen. Figure 3 shows the nonbonding valence σ orbitals present in the YH^+ and TcH^+ (singly occupied s–d_{z^2} hybrids) and CdH^+ (doubly occupied d_{z^2} orbital) molecules. The metal–hydrogen bonds of all second-row elements are fairly covalent with an average transfer of 0.08 electron to hydrogen. The electron transfer ranges from +0.25 electrons transferred to hydrogen in SrH^+ and YH^+ to −0.12 electron in PdH^+; thus there is a fair increase in electronegativity from Y^+ to Pd^+.

The first-row metals bond to hydrogen predominantly with their 4s orbital rather than the 3d orbitals.[5] In contrast, the second-row transition metals tend to bond with 4d rather than 5s electrons (see Table I). AgH^+ is not included in the table due to the fact

0002-7863/87/1509-5565$01.50/0

Table II. Spectroscopic Properties of Ground-State MH^+

molecule	state	bond length R_e, Å	force const,[g] hartree/Å^2	vibrational freq ω_e, cm^{-1}	bond energies, kcal/mol: theory[a] D_e	theory[a] D_0	theory[a] D_{298}	expt D_0[b]	expt D_0[c]
SrH^+	$^1\Sigma^+$	2.079	0.2457	1346	46.0	44.1	45.0		
YH^+	$^2\Sigma^+$	1.892	0.3645	1639	60.1	57.8	58.7		58 ± 3
ZrH^+	$^3\Phi^\pm$	1.857	0.3731	1658	57.0	54.6	55.5		54 ± 3
NbH^+	$^4\Delta^\pm$	1.764	0.4425	1805	51.3	48.7	49.6		53 ± 3
MoH^+	$^5\Sigma^+$	1.708	0.4530	1826	33.8	31.2	32.1		41 ± 3
TcH^+	$^6\Sigma^+$	1.719	0.4099	1737	48.8	46.3	47.2		
RuH^+	$^3\Sigma^-$	1.581	0.5361	1986	34.5	31.7	32.6	40 ± 3.5	
RhH^+	$^2\Delta^\pm$	1.539	0.6138	2125	37.8	34.8	35.7	41 ± 3.5	
PdH^+	$^1\Sigma^+$	1.512	0.6323	2127	43.7	40.6	41.5	44 ± 3.5	53 ± 3
AgH^+	$^2\Sigma^+$	2.428	0.0186	372	2.6	2.1	3.0		15 ± 3
CdH^+	$^1\Sigma^+$	1.709[d]	0.3912	1696[e]	44.4	42.0	42.9		49.3[f]

[a] Present work (GVB-DCCI). [b] Reference 9. D_{298} values have been decreased by 0.9 kcal/mol to give D_0 values. [c] Reference 10. [d] Experimental value 1.67 Å. Reference 8. [e] Experimental value 1771 cm^{-1}. Reference 8. [f] Reference 8. [g] Multiply by 4.359 to obtain mdyn/Å or by 627.5 to obtain (kcal/mol)/Å^2.

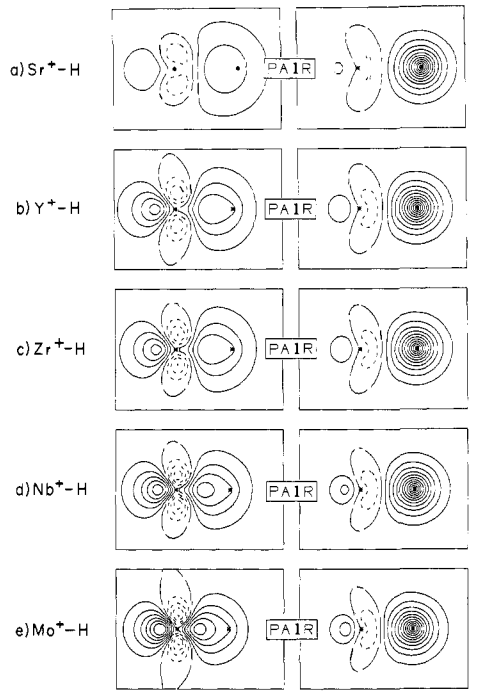

Figure 1. GVB bond orbitals (at R_e) for (a) $^1\Sigma^+$ SrH^+, (b) $^2\Sigma^+$ YH^+, (c) $^3\Phi$ ZrH^+, (d) $^4\Delta$ NbH^+, and (e) $^5\Sigma^+$ MoH^+. Solid lines indicate positive amplitude, dotted lines indicate negative amplitude, and long dashed lines indicate zero amplitude. The spacing between contours is 0.05 au. The contours are plotted in the xz plane with the M^+–H bond axis along the z axis. The plot limits are −2.0 to +3.5 Å for the z axis and −2.0 to +2.0 Å for the x axis.

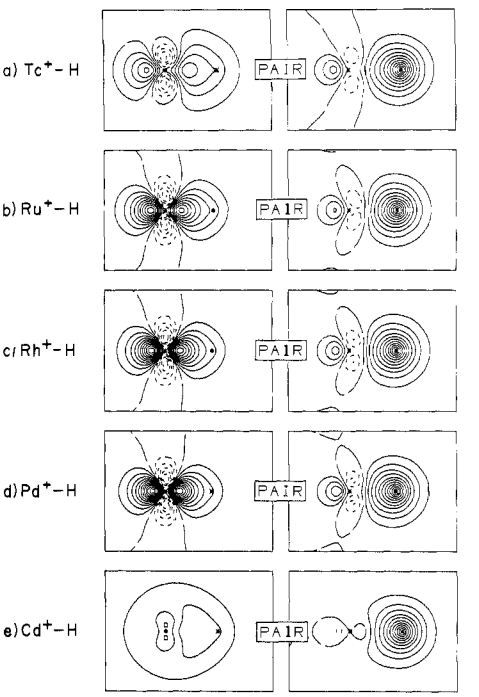

Figure 2. GVB bond orbitals (at R_e) for (a) $^6\Sigma^+$ TcH^+, (b) $^3\Sigma^-$ RuH^+, (c) $^2\Delta$ RhH^+, (d) $^1\Sigma^+$ PdH^+, and (e) $^1\Sigma^+$ CdH^+. All plotting parameters are the same as in Figure 1.

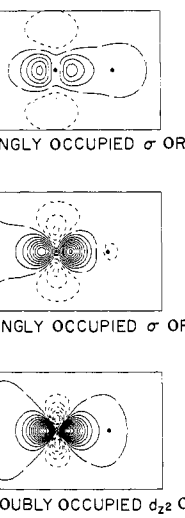

Figure 3. Nonbonding sigma orbitals for (a) $^2\Sigma^+$ YH^+ (66.9% s, 2.9% p, and 30.2% d), (b) $^6\Sigma^+$ TcH^+ (31.5% s, 0.4% p, and 68.1% d), and (c) $^1\Sigma^+$ CdH^+ (0.8% s, 0.1% p, and 99.1% d). All plotting parameters are the same as in Figures 1 and 2.

that the AgH^+ bond arises from an ion–dipole type interaction which does not lead to a "normal" pair of bonding electrons. With the exception of SrH^+ and CdH^+ all species studied have over 50% d character in the metal bonding orbital (92.8% in the case of PdH^+).

Electronic Configuration. In order to understand the trends it is important to keep in mind the number of nonbonding d electrons on the metal, and we will thus indicate the nonbonding orbital occupation in parentheses. Thus, TcH^+ (d^5) indicates five electrons in nonbonding orbitals (coupled high spin). For ZrH^+ (d^2) through PdH^+ (d^8), all but one case have the nonbonding d electrons in $d\pi$ or $d\delta$ orbitals (see Table IX) so that the metal $d\sigma$ and s orbitals are free to mix in forming the bond pair. The exception is TcH^+ (d^5), where the exchange coupling stabilizes the high-spin state having a nonbonding $d\sigma$ electron. AgH^+ (d^9) necessarily has a $d\sigma$ orbital. YH^+ (d^1) also has a $d\sigma$ nonbonding electron for reasons discussed below.

Spectroscopic Properties. The spectroscopic properties calculated for the metal hydrides (bond length, vibrational frequency,

Table III. Valence Orbital Sizes (Å) for Second-Row Transition-Metal Ions [$R = (\langle\phi|r^2|\phi\rangle)^{1/2}$]

		R(4d)				change on bonding MH^+	
		$4d^{n-1}5s^1$		$4d^n$			
ion	R(5s)	$(1e^-)^a$	$(2e^-)^a$	$(1e^-)^a$	$(2e^-)^a$	$R_e - R$(5s)	$R_e - R$(4d)
Sr^+	2.37			1.93		−0.29	0.15
Y^+	2.14	1.38		1.47		−0.25	0.42
Zr^+	2.00	1.21		1.30		−0.14	0.56
Nb^+	1.94	1.11		1.17		−0.18	0.59
Mo^+	1.87	1.02		1.06		−0.16	0.65
Tc^+	1.79	0.95		0.99	1.04	−0.07	0.73
Ru^+	1.72	0.88	0.91	0.93	0.96	−0.14	0.65
Rh^+	1.68	0.84	0.85	0.87	0.89	−0.14	0.67
Pd^+	1.64	0.80	0.80	0.82	0.85	−0.13	0.69
Ag^+	1.64	0.75	0.76		0.80	0.79	
Cd^+	1.60		0.73			0.1	

[a] $1e^-$ and $2e^-$ indicate singly and doubly occupied orbitals.

ground-state symmetry, and bond dissociation energies) are given in Table II.

Bond Lengths. The trend in bond lengths for the second-row metal hydrides (Table III) parallels that for the first-row metal hydrides[5] (with the exception of AgH^+). The bond lengths decrease a total of 0.5 Å as one moves from SrH^+ to PdH^+. As indicated in Table III, this follows the trend of decreasing size in the metal orbitals. Indeed, the MH^+ bond length is systematically about 0.17 Å smaller than the M^+ 5s orbital. Three exceptions to this decreasing bond length are TcH^+ (d^5), CdH^+ (d^{10}), and AgH^+ (d^9). The increase in bond length upon reaching Tc^+ and Cd^+ is due to the completion of stable half-full or completely full 4d shells (of nonbonding electrons) and the concomitant large increase in s character in the bond. For Ag^+, the d^{10} configuration of the ion is so stable that AgH^+ does not make a covalent bond in its ground state and thus does not fit into the bonding trends. Rather, AgH^+ makes an ion–dipole bond, 50% longer than the bond in PdH^+.

Theoretical calculations have been previously reported for SrH^+ and CdH^+ (Dirac–Fock one-center expansion),[6] yielding bond lengths 2.10 and 1.82 Å, respectively, in reasonable agreement with our values of 2.08 and 1.71 Å. For AgH^+ Preuss et al.[7] (using a one valence electron effective core potential for Ag but allowing for core polarization effects) calculate a bond length for AgH^+ of 2.24 Å (we obtain 2.43 Å). Only for CdH^+ is there an experimental bond length,[8] 1.667 Å, in comparison with our value of 1.709 Å and the Pyykkö value of 1.82 Å. The calculated bond length should decrease as further electron correlation is included, and our theoretical values are probably generally about 0.03 Å too long.

Vibrational Frequencies. The vibrational frequency for a bond is often considered to increase with bond strength; however, no such correlation is seen between various transition-metal hydrides. The vibrational frequencies do follow an inverse correlation with the length of the metal–hydrogen bond. Proceeding from SrH^+ (d^0) (2.079 Å, 1346 cm^{-1}), the vibrational frequency increases as the bond length decreases, reaching a maximum for PdH^+ (d^8) (1.512 Å, 2127 cm^{-1}). Again, discontinuities in the smooth increase of the vibrational frequencies are seen for TcH^+ (d^5), AgH^+ (d^9), and CdH^+ (d^{10}), corresponding to the bond length discontinuities. Thus, higher vibrational frequencies are seen for shorter bonds, not necessarily for stronger ones. As with the bond lengths, the vibrational frequency is known experimentally for only CdH^+.[8] The spectroscopic value of 1772 cm^{-1} is 4.5% larger than the theoretical value of 1691 cm^{-1} (consistent with the shorter experimental bond length). It is reasonable to assume that our theoretical vibrational frequencies are also 5% too low for the other systems.

(6) Pyykkö, P. *J. Chem. Soc., Faraday Trans. 2* **1979**, *75*, 1256.
(7) Stoll, H.; Fuentealba, P.; Dolg, M.; Flad, J.; Szentpály, L. V.; Preuss, H. *J. Chem. Phys.* **1983**, *79*, 5532.
(8) Huber, K. P.; Herzberg G. *Constants of Diatomic Molecules*; Van Nostrand Reinhold: New York, 1979.

Table IV. Total Energies for Ground-State MH^+ (at R_e), M^+, and H

		total energy,[a] hartrees		
species	state	GVB-PP	DCCI-GEOM	DCCI
SrH^+	$^1\Sigma^+$	−30.481 47	−30.495 60	−30.495 60
Sr^+	^2S	−29.923 10	−29.923 10	−29.923 10
YH^+	$^2\Sigma^+$	−37.852 32	−37.867 48	−37.870 67
Y^+[b]	^3D	−37.268 55	−37.268 55	−37.269 74
ZrH^+	$^3\Phi^\pm$	−46.356 35	−46.372 77	−46.377 20
Zr^+	^4F	−45.785 47	−45.785 69	−45.787 14
NbH^+	$^4\Delta^\pm$	−56.021 95	−56.941 32	−56.048 40
Nb^+	^5D	−55.460 08	−55.460 08	−55.467 32
MoH^+	$^5\Sigma^+$	−67.202 65	−67.225 31	−67.232 92
Mo^+	^6S	−66.672 12	−66.672 12	−66.679 81
TcH^+	$^6\Sigma^+$	−79.707 81	−79.733 03	−79.743 50
Tc^+	^7S	−79.163 02	−79.163 02	−79.166 44
RuH^+	$^3\Sigma^-$	−93.393 60	−93.439 20	
Ru^+	^4F	−92.881 43	−92.884 07	−92.897 14
RhH^+	$^2\Delta^\pm$	−108.992 31	−109.019 12	−109.031 92
Rh^+	^3F	−108.457 12	−108.458 03	−108.472 33
PdH^+	$^1\Sigma^+$	−126.176 78	−126.200 89	−126.214 56
Pd^+	^2D	−125.628 86	−125.629 41	−125.645 62
AgH^+	$^2\Sigma^+$	−145.167 05		−145.168 06
Ag^+	^1S	−144.663 17		−144.664 60
CdH^+	$^1\Sigma^+$	−46.856 35	−46.871 06	−46.889 90
Cd^+	^2S	−46.299 16	−46.300 65	−46.319 82
H	^2S	−0.499 28	−0.499 28	−0.499 28

[a] For MH^+ the total energies are for the calculation levels shown while the M^+ and H total energies are for the calculation levels to which these MH^+ molecules dissociate (see Calculational Details of text). [b] The $^2\Sigma^+$ state of YH^+ does not dissociate to ground-state Y^+ (^1S) but to ^3D Y^+ as shown here.

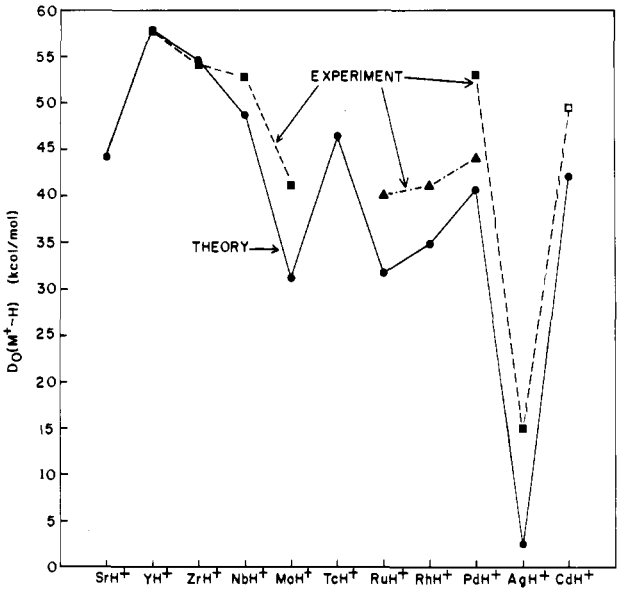

Figure 4. Comparison of experimental and theoretical bond dissociation energies [$D_0(M^+-H)$]: present work (circles); Mandich, Halle, and Beauchamp—ref 9 (triangles); Elkind and Armentrout—ref 10 (closed squares); and Huber and Herzberg—ref 8 (open square).

Bond Dissociation Energies. Total energies for the metal hydrides (at R_e) for three calculation levels (GVB-PP(1/2), DCCI-GEOM, and DCCI) are shown in Table IV. Comparisons of the present theoretical results and the available experimental bond dissociations energies are shown in Table II and in Figure 4. Just as for the first-row metal hydrides, the trend in the bond energies can be understood in terms of the balance between s and d bonding and the character of the ground state; however, these trends are *not* obvious from a plot such as Figure 4. The highest bond energies occur for the very early metals Y^+ (d^1), Zr^+ (d^2), and Nb^+ (d^3) where (i) the s and d orbitals are close in size and energy and readily hybridized and (ii) there is little exchange energy lost on bonding. The smallest bond energy is found for AgH^+ due to the closed-shell d^{10} configuration of Ag^+ and the

high promotional energy just to obtain a state (s^1d^9 configuration) with singly occupied orbitals. The bonding thus results from small ion–dipole interactions rather than normal covalent bonding. The bond energies of other systems oscillate between these two extremes.

For the first-row metal hydrides,[5] our theoretical bond dissociation energies compare very well with the ion beam results of Elkind and Armentrout[10] with an average difference of 2.5 kcal/mol. The overall bond energy trends for the second-row metal hydrides correspond fairly well between experiment and theory, but the actual quantitative values differ more substantially than for the first row. Although the experimental and theoretical results for YH^+ and ZrH^+ are within 1 kcal/mol, the average difference between the present results and the experimental values is 6.7 kcal/mol. However, we should emphasize two points. First, inclusion of f functions on the metal (tested in the case of MoH^+) can increase the theoretical values by as much as 3 kcal/mol. Second, the experimental bond energies for these systems involve analysis of the threshold for $M^+ + H_2 \rightarrow MH^+ + H$ and require correction for excited M^+ in the beam. As a result, reanalysis of the experiments for the first-row metal hydrides has led to decreases of up to 5 or even 10 kcal/mol in some of the experimental values. Thus, the present results, representing a consistent set of calculations for all of the second-row metals, may help with the analysis of experimental results (which are less complete than for the first-row counterparts).

Other theoretical bond dissociation energies have been reported for SrH^+ (81.6 kcal/mol vs. our value of 45.0 kcal/mol),[6] CdH^+ (33.9 kcal/mol vs. our value of 42.9 kcal/mol and the experimental value of 49.3 kcal/mol),[6] and AgH^+ (6.7 kcal/mol vs. our value of 3.0 kcal/mol and an experimental value of 15 ± 3 kcal/mol).[7] Recent calculations by Pettersson et al.[11] on YH^+ through AgH^+ yield bond dissociation energies that are very comparable for the early metal hydrides. For the later metal hydrides their bond energies are from 4 to 7 kcal/mol larger than those in the present study.

Analysis of the Metal–Hydrogen Bond. The major factors affecting the bonding of hydrogen to the second-row metal ions are (1) the orbital character of the low-lying metal electronic states, (2) the relative sizes of the metal s and d orbitals, (3) the intrinsic bond strengths to pure s or d orbitals, (4) the effects of changes in exchange energy of the nonbonding d orbitals, and (5) the effects of metal orbital hybridization.

Low-Lying Metal Electronic States. To analyze the low-lying electronic states, we start with the orbital configuration of the ground electronic state of the ion. This generally involves either a d^n or $d^{n-1}\ s^1$ valence electronic configuration.[12] Our working hypothesis is that the ground configuration or a low-lying excited configuration must have a singly occupied s orbital in order to make an s-like bond or a singly occupied d orbital to make a d-like bond (for Y^+, the ground-state electronic configuration is s^2, but the ^3D state (s^1d^1) is only 0.16 eV higher in energy).[11] Figure 5 shows the relative difference in energy between the lowest electronic states formed from the $4d^n$ and $4d^{n-1}5s^1$ configurations for the second-row transition metals. The general trend is for the state with the d^n configuration to be stabilized, with respect to the state with the $d^{n-1}\ s^{-1}$ configuration, as one proceeds from left to right. Starting with Tc^+ the d^n configuration requires doubly occupying one of the d orbitals leading to an increase of electron–electron repulsion energy and a jump in the $d^n - d^{n-1}\ s^1$ separation.

The 5s orbital is more stable than 4d at the left of the row, but proceeding to the right leads to continuous stabilization of the d orbitals with respect to the s orbital due to differential shielding effects of 4d vs. 5s. The d^n configurations are also stabilized due to larger d–d exchange energies as compared to s–d exchange. These exchange effects are greatest for the half-filled (d^5) and fully-filled (d^{10}) shells. Thus, for Ag^+, the ^1S (d^{10}) state is over 5 eV lower in energy than the ^3D (d^9s^{-1}) state.

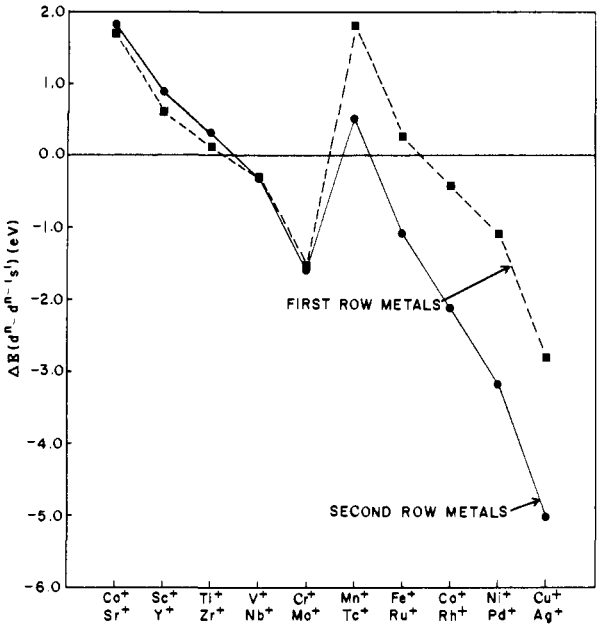

Figure 5. Trends in the difference in energy between the lowest metal electronic states arising from $4d^n$ and $4d^{n-1}5s^1$ configurations for the second-row transition-metal monopositive ions.[12] $\Delta E = E_{d^n} - E_{d^{n-1}s^1}$.

Metal Orbital Sizes. The size of the metal orbitals is intimately related to the shielding by electrons in other orbitals (the effective nuclear charge) and thus to the electronic configuration and relative energies of the electronic states. The relative energy between the lowest electronic states with d^n and $d^{n-1}s^1$ configurations for the late transition metals of the second row increases much more rapidly than for the first row. This is largely due to the reduced electron–electron repulsion resulting from the increased size of the second row d orbitals.

The size of the metal orbital also affects its overlap with a neighboring H atom, which should also affect the bond energies. Table III shows the root-mean-square radii found from Hartree–Fock wave functions for the atomic metal ions. As expected, both s and d orbitals contract in size going from left to right along the row, but the d orbitals contract faster. The ratio of size (R_s/R_d) for Sr^+ is 1.23 while for Ag^+ it is 2.18. In comparison, the first row metals Ca^+ and Cu^+ have size ratios of 1.33 and 2.81, respectively.[5] This results in average differences between orbital sizes for first- and second-row metals of 0.13 Å for s orbitals and 0.30 Å for d orbitals (second row orbitals larger). Thus, for the second row, the size of d orbitals with respect to s is larger than for the first. As shown in Table III, the bond distances of MH^+ track very well with changes in the size of the metal s orbitals. Thus, for SrH^+ through PdH^+ (all of which have significant d character), the MH^+ bond distance averages about 0.17 Å shorter than the size of the s orbital. For CdH^+ with *no* d character, the bond is 0.11 Å larger than the size of the s orbital. Similarly, for YH^+ through PdH^+, the bond distance averages about 0.62 Å larger than the size of the d orbital.

Intrinsic Bond Strengths. It is useful to establish an intrinsic bond strength for the MH^+ bond by making corrections for the energy required to promote the metal to the bonding state and for the exchange energy changes due to the nonbonding orbitals. In order to establish the trends in bond energy to s and d orbitals, we carried out calculations on the metal hydrides in which the mixing of s and d character in the bond was not allowed. The results are tabulated in Table V and presented graphically in Figure 6. The intrinsic s bond is fairly constant over the whole range of metals, increasing approximately 10 kcal/mol between SrH^+ and CdH^+. The discontinuities seen between MoH^+ and TcH^+ and again between AgH^+ and CdH^+ are due to occupation

(9) Mandich, M. L.; Halle, L. F.; Beauchamp, J. L. *J. Am. Chem. Soc.* **1984**, *106*, 4403.
(10) Elkind, J. L.; Armentrout, P. B. *Inorg. Chem.* **1986**, *25*, 1080.
(11) Pettersson, L. G. M.; Bauschlicher, C. W., Jr.; Langhoff, S. R.; Partridge, H., private communication.
(12) Moore, C. E. *Atomic Energy Levels*; National Bureau of Standards: Washington, D.C., 1971; Vols. II and III.

Table V. Intrinsic Bond Dissociation Energies[a]

molecule	s bond kcal/mol	d bond, kcal/mol
SrH^+	26.8	75.0
YH^+	29.7	61.2
ZrH^+	28.9	54.5
NbH^+	29.5	48.5
MoH^+	32.7	40.7
TcH^+	21.1	39.0
RuH^+	23.0	33.9
RhH^+	23.8	32.7
PdH^+	25.2	30.5
AgH^+	25.6	0.0
CdH^+	36.4	0.0

[a] The trends in these numbers should be valid. However, in order to extract separate contributions, restrictions were made in the wave functions that make all numbers too low by ~10–15 kcal/mol.

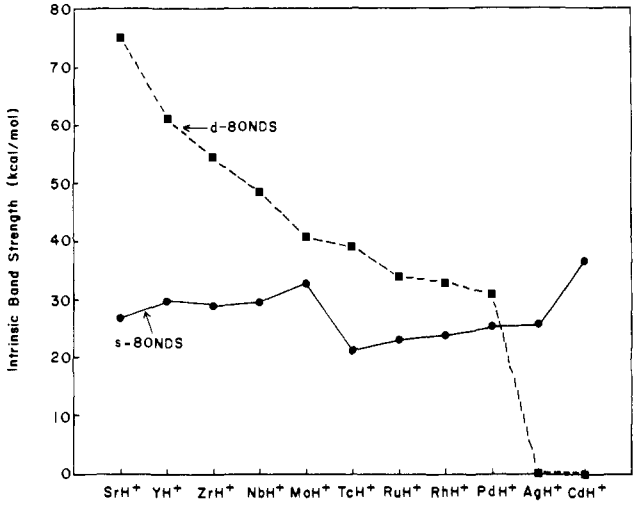

Figure 6. Intrinsic bond strengths of H to metal 5s (circles) and 4d (squares) orbitals from GVB-PP(1/2) calculations. The intrinsic bond energies are the diabatic bond dissociation energies of the complex (allowing no hybridization) adding back in any exchange energy lost on bonding.

of a $d\sigma$ nonbonding orbital to which the bond pair must become orthogonal. The intrinsic d bonding, on the other hand, varies considerably with a value of 75.0 kcal/mol for SrH^+ vs. 30.8 kcal/mol for PdH^+. The decreasing intrinsic d bond strength on moving across the row seems to indicate that the optimum size for a d orbital for bonding H is at least 1.9 Å. The intrinsic s bond trend implies that the optimum size of a 5s orbital for bonding H is smaller than that of Cd^+ (less than 1.6 Å). It should be emphasized here that to exact such the intrinsic bond energies we used GVB-PP(1/2) calculations; thus, the relative values and trends should be reliable, but quantitative values should be too small by ~10–15 kcal/mol.

Exchange Energy Considerations. Loss of exchange energy plays an important role in moderating the bond energies to high-spin species.[13] When a singly occupied orbital of a high-spin atom is used in a bond, the spin coupling in the new bond is such that this orbital has the same spin as the nonbonding orbitals only half the time. Thus, approximately half of the exchange energy between the bonding electron and the other high-spin electrons on the atom is lost, effectively lowering the bond energy. This effect is largest for elements with the highest numbers of high-spin coupled electrons, i.e., toward the middle of the row.

The exchange energy between two electrons is inversely proportional to the average distance between the electrons and thus depends on the orbitals sizes. The d–d exchange energies (K_{dd}) are consistently much larger than the s–d exchange energies (K_{sd}). Consider, for example, Y^+ and Pd^+. The ^3D (d^1s^1) state of Y^+ has K_{sd} = 9.87 kcal/mol, while the ^3F ($d\sigma d\delta$) state of Y^+ has K_{dd} = 11.65 kcal/mol. For the ^4F (d^8s^1) state of Pd^+, K_{sd} = 7.15 kcal/mol and $K_{d\sigma d\delta}$ = 21.14 kcal/mol. Thus, as the orbitals become smaller (with the d orbitals contracting faster), the K_{sd} values decrease, while the K_{dd} values increase. [As indicated in Table VI for Tc^+, the exchange energy also varies somewhat with orbital occupation.] Comparing the average K_{dd} and K_{sd} for the ^6S state of Tc^+ (K_{sd} = 8.28 kcal/mol, K_{dd} = 15.32 kcal/mol) to those of Mn^+ (K_{sd} = 4.81 kcal/mol, K_{dd} = 19.81 kcal/mol),[5] we see that for the second row, K_{sd} is larger and K_{dd} is smaller. The smaller d orbital size and larger K_{dd} for the first row is partly responsible for the dominance of s character in the metal–hydrogen bond. For the second row, Table VII shows a change in the intrinsic bond strengths due to loss of exchange energy. Lower K_{dd} values and higher K_{sd} values for the second row tend to favor bonding to d electrons.

Table VI. 5s–4d and 4d–4d Exchange Energies for the ^6S and ^4D States of Tc^+

	^6S ($5s^14d^5$)		^4D ($4d^6$)	
orbitals	no.	$\bar{K}$, kcal/mol	no.	$\bar{K}$, kcal/mol
s–d	5	8.28	0	
d–d (av)	10	15.32	6	15.19
$d\sigma$–$d\pi$	2	11.76	2	11.20
$d\sigma$–$d\delta$	2	18.88	1	17.95
$d\pi$–$d\pi$	1	16.51	1	15.73
$d\pi$–$d\delta$	4	16.51	2	15.66
$d\delta$–$d\delta$	1	9.38	0	

Metal Orbital Hybridization. Table VIII shows the intrinsic bonding after correcting for exchange energy loss and the necessary promotion energies of the metals. We compare these values to those obtained from GVB-PP(1/2) calculations (which allow optimal metal orbital hybridization). For every case, the d-bond energy is larger then the s-bond energy. This coincides, for all cases except SrH^+, with the actual hybridizations shown in Table I. As expected, the bond energies for the hybridized species are greater than for the unhybridized species. For both the first- and second-row metals the strongest bonds are found for those metals whose admixture of s and d character is allowed by the ground-state configuration while species where this is not possible tend to have weaker bonds.

Low-Lying MH^+ Electronic States. For the first-row metal hydrides, one can predict the ground-state configuration by spin pairing the H to a σ electron of the lowest metal state with a $4s^13d^{n-1}$ configuration and then taking into account the intraatomic electrostatic interaction of the nonbonding valence electrons.[5] This predicts the correct ground state even for species in which the lowest metal ion state does not have a $4s^13d^{n-1}$ configuration (e.g. CoH^+ and NiH^+). The increased importance of the d orbitals for the second-row metals shows up as changes in the metal orbital hybridizations and also in the relative energies of some of the MH^+ low-lying electronic states.

As a illustrative example of differences between the first- and second-row metal hydrides we compare TcH^+ and MnH^+. Both of these metals have a ^7S ground state with a d^5s^1 valence electronic configuration. The ^5D (d^6) state for Tc^+ is 0.51 eV higher in energy while for Mn^+ this state is 1.81 eV above the ground state. Both metal hydrides have $^6\Sigma^+$ ground states, however, the metal bond orbital hybridizations are quite different. The d character in the metal bonding orbitals is seen to be 52.5% and 11.2% for Tc^+ and Mn^+ respectively. This difference can be attributed to the factors discussed previously. Comparing the lower limits for the s and d intrinsic bonding in TcH^+ we find that the intrinsic d bond is on the order of 19 kcal/mol stronger than an s bond. If the hydrogen atom is bonded to the s electron of ^7S Tc^+, there will be a loss of approximately 20.7 kcal/mol of exchange energy, while if a bond is formed to a d electron, approximately 34.8 kcal/mol of exchange energy is lost. Taking into account both the difference in exchange energy lost and the difference in intrinsic bond strengths, one would predict close to a 50–50 s/d hybridization. For MnH^+, the lower limit for the intrinsic s bond is 28.2 kcal/mol while the lower limit for the d bond is 18.8

(13) Goddard, W. A., III; Harding, L. B. *Annu. Rev. Phys. Chem.* **1978**, *29*, 363.

Table VII. Intrinsic Bond Strengths after Correction for Exchange Energy Losses

	s bond			d bond		
	exchange loss		$D_s(M^+-H)$,[a]	exchange loss		$D_d(M^+-H)$,[b]
molecule	K_{sd} terms	energy, kcal/mol	kcal/mol	K_{dd} terms	energy, kcal/mol	kcal/mol
SrH^+	0	0.0	26.8	0	0.0	75.0
YH^+	$^1/_2$	4.9	24.8	$^1/_2$	5.8	55.4
ZrH^+	1	9.1	19.8	1	10.8	43.7
NbH^+	$1^1/_2$	13.2	16.3	$1^1/_2$	16.8	31.7
MoH^+	2	16.9	15.8	2	26.9	13.8
TcH^+	$2^1/_2$	20.7	0.4	$1^1/_2$	20.2	18.8
RuH^+	2	14.8	8.4	1	15.3	18.6
RhH^+	$1^1/_2$	10.9	12.9	$^1/_2$	10.2	22.5
PdH^+	1	7.2	18.0	0	0.0	30.5
AgH^+	$^1/_2$	5.9	19.7	0	0.0	0.0
CdH^+	0	0.0	36.4	0	0.0	0.0

[a] $D_s(M^+-H)$ = (intrinsic s-bond energy) − (exchange energy lost on bonding to s orbital). [b] $D_d(M^+-H)$ = (intrinsic d-bond energy) − (exchange energy lost on bonding to dσ orbital).

Table VIII. Comparison of s, d, and Hybridized Bonding in MH^+

	intrinsic bond energies after corrections for exchange and promotion energies[a]		calcd bond energies[b] (no restrictions),
molecule	s bond, kcal/mol	d bond, kcal/mol	kcal/mol
SrH^+	26.8	32.8	37.1
YH^+	24.8	35.1	49.3
ZrH^+	19.8	36.6	44.9
NbH^+	8.7	31.7	39.3
MoH^+	−20.9	13.8	19.6
TcH^+	0.4	7.0	28.6
RuH^+	−16.9	18.6	18.6
RhH^+	−36.2	22.5	22.5
PdH^+	−55.6	30.5	30.5
AgH^+	−95.9	0.0	0.0
CdH^+	36.4		36.4

[a] Bond energy = (intrinsic bond strength) − (exchange energy lost on bonding) − (metal promotion energy). [b] GVB perfect pairing wave function with no restrictions on orbital hybridization.

kcal/mol. Thus, there is a reversal between the two bonds for the first- and second-row species. Again looking at bonding H to the ^7S state, one would predict a loss of 12 kcal/mol on bonding to an s electron and 42 kcal/mol on bonding to a d_{z^2} electron. Thus, for Mn^+, s character in the bond is overwhelmingly favored from the standpoint of both the intrinsic bond energies and the loss of exchange energy. An important point to note from the TcH^+ results is that s–d_{z^2} hybridization can and does take place when bonding an H atom to a metal state which contains singly occupied s and d_z orbitals. The two metal orbitals can be hybridized to form two orbitals, one of which has electron density primarily located along the z axis and the other of which has electron density located in a torus in the xy plane. Orbitals of this type can be seen in the orbital plots (Figures 1–3).

The lowest lying electronic states for the two MH^+ species are quintet states formed by bonding the hydrogen to the d^6 configuration of the metal. For TcH^+, the $^5\Delta$ and $^5\Pi$ states are found at 25.1 and 37.2 kcal/mol, respectively, above the ground state. For MnH^+, the state splittings have not been calculated; however, due to the lower bond strength to the Mn d_{z^2} orbital and the 1.3-eV increase in the metal promotion energy, these states are expected to be much higher in energy than seen for the TcH^+ molecule.

The splitting between the lowest lying electronic states of Zr^+ (d^2), Nb^+ (d^3), and Mo^+ (d^4) is similar to that for Ti^+, V^+, and Cr^+, and as expected the ordering of states is similar. For these early transition metals, the bonding metal orbitals use large amounts of both s and d character (as seen in TcH^+). For metals where the difference in energy of states with d^n and s^1d^{n-1} configurations is fairly small, this hybridization will usually come from a mixing of the two configurations. For these configurations to be compatible, the s^1d^{n-1} configuration must have an empty d_{z^2} orbital, but this is possible for each of these metals. Indeed, even the order of the low-lying excited states can often be predicted from examining the optimum states for the s^1d^{n-1} configurations of the ion and determining whether the d_{z^2} orbital is empty, as will be examined next.

For Zr^+, examining the d shell, the d^2 (^3F) configuration leads to seven states of ^3F symmetry, which, in terms of real d orbitals, can be written as

$$\begin{aligned}
\Phi^+&: [d_{xz}d_{x^2-y^2} - d_{yz}d_{xy}]\\
\Phi^-&: [d_{xz}d_{xy} + d_{yz}d_{x^2-y^2}]\\
\Delta^+&: [d_{z^2}d_{x^2-y^2}]\\
\Delta^-&: [d_{z^2}d_{xy}]\\
\Pi^+&: \{(3/5)^{1/2}[d_{xz}d_{x^2-y^2} + d_{yz}d_{xy}] + (2/5)^{1/2}[d_{z^2}d_{xz}]\}\\
\Pi^-&: \{(3/5)^{1/2}[d_{xz}d_{xy} - d_{yz}d_{x^2-y^2}] + (2/5)^{1/2}[d_{z^2}d_{yz}]\}\\
\Sigma^-&: \{(4/5)^{1/2}[d_{xz}d_{yz}] + (1/5)^{1/2}[d_{x^2-y^2}d_{xy}]\}
\end{aligned} \quad (1)$$

Of these, only the $^3\Phi$ and $^3\Sigma^-$ states have an empty d_{z^2} orbital, and hence we expect them to be lower in energy. The $^3\Phi$ state should be lower since one nonbonded electron is always π-like and the other δ-like, while in the $^3\Sigma^-$ state 80% of the time the two electrons are both in the π orbitals (increasing the electron–electron repulsion with the bond pair) and 20% of the time they are both in the δ orbitals which place the two electrons in the same plane. On the basis of the d_{z^2} occupations, one would expect the $^3\Pi$ state next highest in energy, with the $^3\Delta$ state higher yet. This ordering is correct except that the $^3\Delta$ state is actually lower in energy than the $^3\Sigma^-$ state. The electronic configurations for the $^3\Delta$ states involve singly occupied s and d_{z^2} orbitals which can mix as seen in TcH^+. However, occupation of a nonbonding σ orbital leads to higher electron–electron repulsion with the bonding electrons. Thus, although the $^3\Delta$ states can add in d character without use of the excited-state configuration, the increased electron–electron repulsion raises the energy sufficiently such that the $^3\Phi$ state is the ground state.

For Nb^+, the three electrons of the d shell lead to seven ^4F states:

$$\begin{aligned}
\Phi^+&: \{d_{z^2}[d_{xz}d_{x^2-y^2} - d_{yz}d_{xy}]\}\\
\Phi^-&: \{d_{z^2}[d_{xz}d_{xy} + d_{yz}d_{x^2-y^2}]\}\\
\Delta^+&: [d_{xz}d_{yz}d_{xy}]\\
\Delta^-&: [d_{xz}d_{yz}d_{x^2-y^2}]\\
\Pi^+&: \{(3/5)^{1/2}[d_{z^2}[d_{xz}d_{x^2-y^2} + d_{yz}d_{xy}]] + (2/5)^{1/2}[d_{yz}d_{x^2-y^2}d_{xy}]\}\\
\Pi^-&: \{(3/5)^{1/2}[d_{z^2}[d_{xz}d_{xy} - d_{yz}d_{x^2-y^2}]] + (2/5)^{1/2}[d_{xz}d_{x^2-y^2}d_{xy}]\}\\
\Sigma^-&: \{(4/5)^{1/2}[d_{z^2}d_{x^2-y^2}d_{xy}] + (1/5)^{1/2}[d_{z^2}d_{xz}d_{yz}]\}
\end{aligned} \quad (2)$$

Here the ordering of states can be predicted on the basis of d_{z^2} occupation in the s^1d^{n-1} configurations ($^4\Delta^\pm < {}^4\Pi^\pm < {}^4\Sigma^- < {}^4\Phi^\pm$), leading to a $^4\Delta$ ground state. This sequence is the same as that

Table IX. Relative Energies for Some Low-Lying Metal Hydride Electronic States

molecule	state	nonbonding configuratn dσ	dπ	dδ	R_e, Å	ω_e, cm^{-1}	force constant,[a] hartrees/Å^2	rel energy, kcal/mol
SrH^+	$^1\Sigma^+$	0	0	0	2.079	1346	0.2457	0.0
YH^+	$^2\Sigma^+$	1	0	0	1.892	1639	0.3645	0.0
	$^2\Delta^{\pm}$	0	0	1	1.954	1554	0.3275	8.3
	$^2\Pi^{\pm}$	0	1	0	1.949	1530	0.3176	15.2
ZrH^+	$^3\Phi^{\pm}$	0	1	1	1.857	1658	0.3731	0.0
	$^3\Delta^{\pm}$	1	0	1	1.843	1680	0.3830	1.5
	$^3\Sigma^-$	0	2	0	1.866	1658	0.3729	2.3
		0	0	2				
	$^3\Pi^{\pm}$	0	1	1	1.856	1655	0.3717	3.8
		1	1	0				
NbH^+	$^4\Delta^{\pm}$	0	2	1	1.764	1805	0.4425	0.0
	$^4\Pi^{\pm}$	0	1	2	1.788	1763	0.4220	1.9
		1	1	1				
	$^4\Sigma^-$	1	2	0	1.808	1673	0.3800	8.7
		1	0	2				
	$^4\Phi^{\pm}$	1	1	1	1.780	1719	0.4012	10.0
MoH^+	$^5\Sigma^+$	0	2	2	1.708	1826	0.4536	0.0
	$^5\Delta^{\pm}$	1	2	1	1.728	1752	0.4170	25.1
	$^5\Pi^{\pm}$	1	1	2	1.730	1711	0.3977	37.2
TcH^+	$^6\Sigma^+$	1	2	2	1.719	1737	0.4099	0.0
	$^4\Delta^{\pm}$	0	2	3	1.664	1886	0.4831	24.0
	$^4\Pi^{\pm}$	0	3	2	1.641	1879	0.4796	26.4
RuH^+	$^3\Sigma^-$	0	4	2	1.581	1986	0.5361	0.0
		0	2	4				
	$^3\Phi^{\pm}$	0	3	3	1.601	1932	0.5070	0.2
	$^5\Delta^{\pm}$	1	2	3	1.696	1775	0.4283	6.7
	$^3\Pi^{\pm}$	0	3	3	1.614	1869	0.4747	9.0
	$^5\Pi^{\pm}$	1	3	2	1.664	1828	0.4541	9.0
	$^5\Sigma^+$	2	2	2	1.711	1733	0.4081	15.7
RhH^+	$^2\Delta^{\pm}$	0	4	3	1.539	2125	0.6138	0.0
	$^2\Pi^{\pm}$	0	3	4	1.588	1716	0.4002	19.5
PdH^+	$^1\Sigma^+$	0	4	4	1.512	2127	0.6323	0.0
AgH^+	$^2\Sigma^+$	1	4	4	2.428	372	0.0186	0.0
	$^2\Delta^{\pm}$	2	4	3	1.745	1587	0.3424	80.3
	$^2\Pi^{\pm}$	2	3	4	1.782	1553	0.3279	81.5
CdH^+	$^1\Sigma^+$	2	4	4	1.709	1696	0.3912	0.0

[a] Multiply by 4.359 to obtain mdyne/Å or by 627.5 to obtain (kcal/mol)/Å^2.

for VH^+. The s–d_{z^2} hybridization seen for the $^3\Delta$ states of ZrH^+ and the $^6\Sigma$ state of TcH^+ is not important in NbH^+ due to the importance of the d bonding and the presence of a d^4 configuration in the ground state of the metal ion.

For MoH^+, we analyze the bonding using the d orbital occupations for s^1d^4. The d hole can be either dσ, dπ, or dδ leading to $^5\Sigma^+$, $^5\Pi^{\pm}$, and $^5\Delta^{\pm}$ states. The $^5\Sigma$ state is expected to be the ground state since this state can be formed by bonding the hydrogen to either the ground or first excited state of the metal and both d^5 and s^1d^4 configurations of the metal ion can readily mix. The $^5\Pi$ and $^5\Delta$ states are expected to be higher in energy since they cannot be formed by bonding hydrogen to ground-state Mo^+ and require promotion to an excited state of the metal ion (^{6}D–1.59 eV higher in energy than the ^{6}S ground state of Mo^+). Indeed, the $^5\Delta$ state is found to be over 25 kcal/mol above the ground $^5\Sigma^+$ state with the $^5\Pi$ state at over 37 kcal/mol.

Y^+ is the only metal which does not have a ground state with either a d^n or s^1d^{n-1} electronic configuration. The Y^+ ground-state configuration is $5s^2$ with no 4d electrons. One cannot form a bond to the Y^+ ground state without first uncoupling the two s electrons and adding in a higher electronic state of the metal such as the ^{3}P state (s^1p^1). We will thus analyze the bonding in a similar fashion to the other early metals. The ^{3}D (s^1d^1) state of Y^+ lies 0.16 eV above the ground state. The lowest state with a d^2 configuration is 0.88 eV higher in energy. If one considers bonding hydrogen to ^{3}D Y^+, there are three possible symmetries $^2\Delta^{\pm}$, $^2\Pi^{\pm}$, and $^2\Sigma^+$ resulting from placing the nonbonding electron in either the dδ, dπ, or dσ orbitals. The energy ordering is expected to be $^2\Delta < {}^2\Pi < {}^2\Sigma$ as seen for ScH^+, which presumably results from the decreased electrostatic interaction of the δ orbital with the electrons of the bond pair. One might have expected the dσ to be stabilized because of less shielding, but it must also be orthogonalized to the bond pair. Table IX shows the energy ordering for these three states of YH^+. Although the $^2\Delta$ state is lower than $^2\Pi$, the ground state is $^2\Sigma^+$. There are two reasons for this difference between ScH^+ and YH^+. The most important is the presence of the ^{1}S (s^2) ground state of Y^+ which mixes into the $^2\Sigma$ wave function and lowers the energy. The lowest state of Sc^+ with an s^2 configuration is 1.44 eV above the ground state and thus does not play much of a role. The second factor is the importance of d character in the second-row bonding and the ability to mix singly occupied s and d_{z^2} orbitals as seen for other second-row metals. The bonding orbitals and singly occupied σ orbitals shown in Figures 1 and 3 show this hybridation. The nonbonding orbital shows very few contours in the region of the torous in the *xy* plane due to the very diffuse nature of the 5s orbital.

The second-row group 8–10 hydrides exhibit much different bonding compared with their first-row cogeners. This is basically a consequence of the greater stability of the d^n configuration with respect to the s^1d^{n-1} configuration for the second row (Figure 5). For the first row, the lowest state with an s^1d^{n-1} configuration is 0.25 eV above the lowest state with a d^n configuration for Fe^+. The ordering is reversed for Co^+ and Ni^+ with the d^n configuration lower in energy by 0.43 and 1.09 eV, respectively. For all three second-row metal ions, Ru^+–Pd^+, the d^n configuration is lower with energy differences of 1.09, 2.13, and 3.19. eV, respectively. Due to the stronger intrinsic s bonds for the first-row metals, they bond with an orbital predominantly s in character (the ground state for NiH^+ is the $^3\Delta$ state arriving from bonding to Ni^+ s^1d^8). The second-row groups 8–10 metals bond primarily with d electrons (bonding is to the d^n metal configuration). For RuH^+, the d^7 (^{3}F) configuration leads to the same configuration of singly occupied orbitals as in eq 2, but now we want a singly occupied d_{z^2} orbital for the bond. This leads to $^3\Sigma^-$ and $^3\Phi^{\pm}$ states that are within 0.1 eV. Other triplet states of RuH^+ are higher in energy (the $^3\Pi^{\pm}$ states are at 9.0 kcal/mol) since these have configurations with two electrons in the metal d_{z^2} orbital. The $^5\Delta$ state (the

Table X. The d Basis for Sr^+.[a] Gaussian Primitive Functions with Exponents (α_i) and Contraction Coefficients (C_i)

α_i	C_i
8.186	−0.004 582 513
2.749	0.009 945 296
0.5851	1.000 000 000
0.09465	1.000 000 000

[a] From unpublished calculations by Rappé and Goddard.[14]

ground electronic state for FeH^+), expected to be the lowest of the quintet states, is found at 6.7 kcal/mol above the ground state. The $^5\Pi$ and $^5\Sigma$ states are found at 9.0 and 15.7 kcal/mol, respectively. For RhH^+, the best Rh d^8 (^3F) configuration has singly occupied d_{z^2} and $d\delta$ orbitals leading to a $^2\Delta$ state. For d^9 Pd^+, the only configuration with a singly occupied d_{z^2} orbital leads to a $^1\Sigma^+$ state for PdH^+. The quartet states of RhH^+ and triplet states of PdH^+ are expected to be much higher in energy due to the large d^n to s^1d^{n-1} promotion energies (2.13 and 3.19 eV for Rh^+ and Pd^+, respectively).

Ag^+ has a ^1S (d^{10}) ground state, with the first excited state, ^3D (s^1d^9), 5.03 eV (116 kcal/mol) higher in energy. The states possible for AgH^+ from these two metal configurations are $^2\Sigma^+$, $^2\Pi^{\pm}$, and $^2\Delta^{\pm}$. The $^2\Pi$ and $^2\Delta$ states necessitate bonding to ^3D Ag^+. Although the $^2\Delta$ state has a bond of 38.3 kcal/mol with respect to dissociation to ^3D Ag^+ and ^2S H, this is 77.7 kcal/mol above the ground-state fragments. The $^2\Pi$ states are even higher in energy. A $^2\Sigma^+$ state can be constructed by bonding the H either to a ^1S or ^3D configuration; however, the ^3D state is too high in energy to contribute. The difference in IP's of Ag (7.574 eV) and H (13.595 eV) also rules out a resonant three-electron bond. One is left with a bond arising from interation of the Ag^+ ion and an induced hydrogen dipole, leading to a long (2.428 Å) weak bond of only 2.6 kcal/mol.

For Sr^+ and Cd^+, bonds involve primarily 5s character due to the high promotion energy in Sr^+ and the doubly occupied d_{z^2} orbital of Cd^+.

III. Calculational Details

Basis Sets. In these studies, the 28 electrons associated with the $n = 1$, 2, and 3 metal core orbitals have been replaced with the ab initio effective core potentials of Hay and Wadt[14] which include relativistic effects in the core electrons. Thus the 4s, 4p, 4d, 5s, and 5p electrons are considered explicitly (e.g., 14 electrons for Tc^+). The basis set is contracted valence triple ζ (5s,5p,4d/4s,4p,3d). For Sr^+, the published Hay and Wadt basis does not include d basis functions, and therefore a set of four 4d functions was added and contracted triple ζ (Table X).[15] For Cd^+ we also used the Hay and Wadt[16] effective core potential, where the full Kr core (36 electrons) were replaced by the EP (leaving 11 electrons to be considered explicitly), and this basis was contracted (3s,3p,4d/3s,3p,3d). Table XI shows a comparison between experimental and theoretical state splittings obtained by using these basis sets. For hydrogen, we used the unscaled Dunning/Huzinaga[17] double-ζ basis (4s/2s) supplemented with one set of p polarization functions. The p functions ($\alpha = 0.50$) are the same as those used for calculations of the first-row metal hydrides.[5] No f polarization functions have been included on the metal ions. To estimate the effects on the bond dissociation energies of including f functions, one set of f functions was optimized for MoH^+ ($\alpha = 0.48$) at the optimum geometry and at the DCCI–GEOM level of calculation. The polarization functions were found to increase the bond dissociation energy by about 3 kcal/mol.[18] This same effect would also be expected for the other second-row metal hydrides.

Table XI. Low-Lying $5s^14d^{n-1}$ and $4d^n$ States of Metal Cations: Experimental and Theoretical State Splittings

	$5s^14d^{n-1}$		$3d^n$				
					rel energy,[a] eV		
ion	state	confign	state	confign	exptl[b]	HF	DCCI
Sr^+	^2S	$5s^1$	^2D	$4d^1$	1.83	2.27	2.27
Y^+[c]	^3D	$5s^14d^1$	^3F	$4d^2$	0.88	0.86	0.83
Zr^+	^4F	$5s^14d^2$	^4F	$4d^3$	0.31	0.31	0.17
Nb^+	^5F	$5s^14d^3$	^5D	$4d^4$	−0.33	−0.31	−0.30
Mo^+	^6D	$5s^14d^4$	^6S	$4d^5$	−1.59	−1.82	−1.74
Tc^+	^7S	$5s^14d^5$	^5D	$4d^6$	0.51	1.48	1.22
Ru^+	^6D	$5s^14d^6$	^4F	$4d^7$	−1.09	−0.59	−0.82
Rh^+	^5F	$5s^14d^7$	^3F	$4d^8$	−2.13	−1.61	−1.83
Pd^+	^4F	$5s^14d^8$	^2D	$4d^9$	−3.19	−2.61	−2.64
Ag^+	^3D	$5s^14d^9$	^1S	$4d^{10}$	−5.03	−4.95	−4.90
Cd^+	^2S	$5s^14d^{10}$					

[a] Relative energy of the $4d^n$ state with respect to the $5s^14d^{n-1}$ state. [b] Reference 12. The energies were calculated by using a weighted average over J levels for each state. [c] The ground state of Y^+ is ^1S ($5s^2$) which is 0.16 eV lower in energy than the ^3D state. GVB(1/2) calculations put the ^1S state 0.43 eV higher than the ^3D state.

Wave Functions and Electronic Correlation. Spectroscopic Parameters. For the second-row metal hydrides, the same calculational methods were used as for the first-row metal hydrides. For the M^+–H bond dissociation energies we use the DCCI level of calculation (dissociation consistent configuration interaction). This involves starting with the configurations of a GVB–PP(1/2) wave function (where the bonding electrons form the GVB pair). From a restricted CI in bond pair orbitals (GVB-RCI(1/2)) we allow all single and double excitations from the bond pair *times* all single excitations out of the nonbonded valence orbitals. The molecular calculation dissociates to a limit involving a free H atom plus a metal wave function having simultaneous single excitations out of the nonbonding orbitals and out of the metal σ bonding orbital. The equilibrium geometries and vibrational frequencies were determined at the DCCI-GEOM calculation level. This involves starting with the GVB-RCI(1/2) configurations and allowing all single and double excitations out of the bond pair *plus* all single excitations out of the nonbonding valence orbitals. This calculation dissociates to a Hartree–Fock hydrogen atom and a metal ion with single excitations from the nonbonding orbitals.

For molecular states involving several occupations of the nonbonding orbitals, the GVB calculation was altered to place an average number of electrons in each nonbonded d orbital and thus produce a set of cylindrically symmetric d orbitals. The CI calculation then started with configurations representing all possible occupations of these nonbonding orbitals, allowing the normal level of excitation, and selecting for proper symmetry of the resultant configurations. This allows mixing in of the two or three major configurations necessary for the particular electronic state with no discrimination due to orbital shapes.

For the $^2\Sigma^+$ state of AgH^+, to allow the necessary polarization in the σ system, the calculations were modified. For this d^{10} configuration the GVB pair consists of in/out correlation of the d_{z^2} electrons rather than a "normal" bond pair and has the unpaired electron located on the hydrogen rather than in a metal d orbital. In order to not bias against other bonding configurations, the CI calculation for this molecule involves all triple and lower excitations from these three σ orbitals.

Bond dissociation energies are determined by dissociating the molecules diabatically to H atom and metal ion. For all cases except YH^+, the metal hydrides dissociate smoothly to ground-state fragments and the bond dissociation energy is given by the difference in energy between the molecule at its equilibrium geometry and the energy of the separated atoms in their ground states. For YH^+, the diabatic dissociation limit is the ^3D (s^1d^1) state. The bond energy is thus taken to be this diabatic dissociation energy minus the experimental state splitting between the ^1S and ^3D states of Y^+. This allows for consistent dissociation of the molecule and cancellation of basis set errors plus the use of the

(14) Hay, J. P.; Wadt, W. R. *J. Chem. Phys.* **1985**, *82*, 299.
(15) Rappé, A. K.; Goddard, W. A., III, to be submitted for publication.
(16) Hay, J. P.; Wadt, W. R. *J. Chem. Phys.* **1985**, *82*, 270.
(17) (a) Huzinaga, S. J. *J. Chem. Phys.* **1965**, *42*, 1293. (b) Dunning, T. H., Jr. *J. Chem. Phys.* **1970**, *43*, 2823.
(18) MoH^+ (at R_e) with one set of f functions ($\alpha = 0.48$) has a total energy of −67.229 76 hartrees compared to −67.225 31 hartrees without f functions (at the DCCI-GEOM calculation level). Thus, the increase in the bond dissociation energy is 2.8 kcal/mol.

correct metal state splitting.

Full DCCI calculations for RuH^+ were excessively large and were not performed. The bond energy for RuH^+ was obtained as follows. The difference between the DCCI-GEOM and DCCI bond energies for other largely "d-bonded" species is 1.6 kcal/mol for PdH^+, 1.0 kcal/mol for RhH^+, and 0.0 kcal/mol for MoH^+ (with the DCCI-GEOM energies larger than the DCCI results). Thus, RuH^+ was assigned a difference of 0.5 kcal/mol which was subtracted from the DCCI-GEOM result.

Intrinsic Bond Dissociation Energies. To obtain intrinsic s-like or d-like bond dissociation energies, the mixing of s and d character must be restricted while allowing other orbital readjustments to occur. The calculation method thus depends on the particular system. For SrH^+–MoH^+, formation of an s bond leads to an empty d_{z^2} orbital while formation of a d bond leads to an empty s orbital. The calculations were thus carried out by eliminating the 5s or $4d_{z^2}$ basis functions. The bond length was then optimized under these conditions and the bond dissociation energy determined by dissociating the molecule to fragments where the same basis functions were removed from the metal ion calculation.

For TcH^+–CdH^+ the state involving an s bond is complicated by the presence of nonbonding σ electrons. The d_{z^2} basis functions could thus not be removed. For TcH^+–AgH^+ the rehybridization process was effectively removed by placing one electron in a d_{z^2} orbital optimized for the corresponding state of the metal ion and freezing this orbital in the predetermined shape while allowing the other orbitals on the molecule to vary. The bonding orbital is thus forced to become orthogonal to the d_{z^2} orbital. For CdH^+ the GVB-PP(1/2) results are used since very little d character is present. The d bonding for TcH^+–PdH^+ is determined by bonding hydrogen to the d^n configuration of the metal, while for AgH^+ and CdH^+ there is effectively no d bonding due to the full d^{10} shell.

These restricted calculations are at the GVB perfect pairing level and *not* the DCCI level used for reliable bond dissociation energies. Only the trends involved should be considered. The actual intrinsic bond energies presented in Table V are obtained from the GVB-PP calculations plus adding in the total amount of s–d or d–d exchange energy lost on bonding (determined from the metal ion exchange energies and the metal electronic configuration) and any electronic promotion energy.

MH^+ Electronic State Splitting Calculations. The relative energies of the low-lying electronic states of the metal hydride ions are determined by the difference in bond dissociation energies calculated for the various states at the DCCI-GEOM level of calculation. The relative bond dissociation energies were used as a measure of energy differences for the electronic states since the dissociation consistent nature of these calculations helps to remove errors inherent in the basis set representations of the metal ion states.

IV. Conclusion

The results presented here for the second-row transition-metal hydrides form a consistent and systematic set of data which should be helpful both for understanding the complex factors involved in metal bonding and as a contribution to the increasing data base of thermodynamic and spectroscopic values for metal compounds. The ideas used to discuss the bonding in the metal hydride diatomics are also applicable for other more complicated metal-containing species. The consistent nature of the data for the entire row should be useful in helping to extract further reliable thermodynamic information from ion beam studies, increase understanding of the differences in reactivity of ground and excited states, and shed light on the reactivity differences of the different transition metals.

Acknowledgment. We thank the National Science Foundation (Grants CHE83-18041 and CHE84-07857) for partial support of this work.

Registry No. SrH^+, 41336-18-9; YH^+, 101200-09-3; ZrH^+, 101200-10-6; MoH^+, 101200-12-8; NbH^+, 101200-11-7; TcH^+, 106520-06-3; RuH^+, 90624-36-5; RhH^+, 90624-38-7; PdH^+, 85625-94-1; CdH^+, 41411-12-5.

Theoretical Studies of Transition-Metal Methyl Ions, MCH_3^+ (M = Sc, Cr, Mn, Zn, Y, Mo, Tc, Pd, Cd)

J. Bruce Schilling, William A. Goddard III,* and J. L. Beauchamp

Contribution No. 7553 from the Arthur Amos Noyes Laboratory of Chemical Physics, California Institute of Technology, Pasadena, California 91125. *Received February 13, 1987*

Abstract: Selected transition-metal methyl cations have been studied by using ab initio generalized valence bond and configuration interaction methods. We present equilibrium geometries and bond dissociation energies and analyze the character of the wave function for the ground-state MCH_3^+ species. The present calculations are compared with previous studies of the corresponding MH^+ molecules. MCH_3^+ is similar to MH^+ from the standpoint of orbital hybridization, electron transfer, bond orbital overlap, and bond dissociation energy. Thus, we find bond energy differences $D(M^+–CH_3) - D(M^+–H)$, ranging from −3.6 kcal/mol for M = Mo to +6.0 kcal/mol for M = Zn, whereas the total bond energy is calculated to range from 24 to 60 kcal/mol. Experimental estimates suggest that $D(M^+–CH_3)$ is, on the average, about 6 kcal/mol larger than $D(M^+–H)$.

I. Introduction

Bond dissociation energies are extremely important in chemistry for use in designing syntheses, predicting stable molecular structures, and predicting and analyzing reaction mechanisms and products. Although a large number of bond energies have been determined for organic compounds, relatively few are known quantitatively for organometallic compounds.[1-6] Even for these few, many of the bond energies are known only as averages of several metal–ligand bonds rather than as a bond energy for a particular metal–ligand bond. Recently, there have been a number of experimental determinations of bond energies for neutral[7,8] and

(1) Conner, J. A. *Top. Curr. Chem.* **1979**, *71*, 71.
(2) (a) Skinner, H. A. *Adv. Organomet. Chem.* **1964**, *2*, 49. (b) Skinner, H. A. *J. Chem. Thermodyn.* **1964**, *10*, 309.
(3) Gaydon, A. G. *Dissociation Energies and Spectra of Diatomic Molecules*; Chapman and Hall, London, 1968.
(4) Huber, K. P.; Herzberg, G. *Molecular Spectra and Molecular Structure. IV. Constants of Diatomic Molecules*; Van Nostrand Reinhold; New York, 1979.
(5) (a) Halpern, J. *Acc. Chem. Res.* **1982**, *15*, 238. (b) Halpern, J. *Inorg. Chim. Acta* **1985**, *100*, 41.
(6) (a) Yoneda, G.; Blake, D. M. *J. Organomet. Chem.* **1980**, *190*, C71. (b) Yoneda, G.; Blake, D. M. *Inorg. Chem.* **1981**, *20*, 67.
(7) Sallans, L.; Kelley, R. L.; Squires, R. R.; Freiser, B. S. *J. Am. Chem. Soc.* **1986**, *107*, 4379.

0002-7863/87/1509-5573$01.50/0